

Excitation and Turbine Neurocontrol with Derivative Adaptive Critics of Multiple Generators on the Power Grid

*†G.K.Venayagamoorthy
Member, IEEE

Department of Electronic
Engineering,
ML Sultan Technikon, POBox 1334
Durban 4000 South Africa
gkumar@ieee.org

*R.G.Harley Fellow, IEEE
School of Electrical and Computer
Engineering
Georgia Institute of Technology
Atlanta GA 30332-0250 USA
ron.harley@ee.gatech.edu

D.C.Wunsch Senior Member,
IEEE

†Applied Computational Intelligence
Laboratory
University of Missouri-Rolla
MO 65409-0249 USA
dwunsch@ece.umr.edu

*Electrical Engineering Department University of Natal Durban 4041 South Africa

Abstract

Based on derivative adaptive critics, neurocontrollers for excitation and turbine control of multiple generators on the electric power grid are presented. The feedback variables are completely based on local measurements. Simulations on a three-machine power system demonstrate that the neurocontrollers are much more effective than conventional PID controllers, the automatic voltage regulators and the governors, for improving dynamic performance and stability under small and large disturbances.

1 Introduction

Power systems containing turbogenerators are large-scale nonlinear systems. The conventional controllers for the generators are designed by linear control theory based on a single-machine infinite bus (SMIB) power system model. These SMIB power system models are linearized at specific operating points, and then excitation and turbine controllers are designed, based on the linearized models. The drawback of this approach is that once the operating point or the system configuration changes, the performance of the controller degrades. Conservative designs are therefore used, particularly in multimachine systems, to attempt satisfactory control over the entire operating range of the power system.

In recent years, renewed interest has been shown in power systems control using nonlinear control theory, particularly to improve system transient stability [1,2]. Instead of using an approximate linear model, as in the design of the conventional power system stabilizer, nonlinear models are used and nonlinear feedback linearization techniques are employed on the power system models, thereby alleviating the operating point dependent nature of the linear designs. Nonlinear controllers significantly improve the power system's transient stability. However, nonlinear controllers have a

more complicated structure and are difficult to implement relative to linear controllers. In addition, feedback linearization methods require exact system parameters to cancel the inherent system nonlinearities, and this contributes further to the complexity of stability analysis. The design of decentralized linear controllers to enhance the stability of interconnected nonlinear power systems within the whole operating region is still a challenging task [3]. However, the use of Artificial Neural Networks offers a possibility to overcome this problem.

Multilayer perceptron type artificial neural networks (ANNs) are able to identify/ model time varying single turbogenerator systems [4] and, with continually online training, these models can track the dynamics of the power system, thus yielding adaptive identification. ANN controllers have been successfully implemented on single turbogenerators using ANN identifiers and indirect feedback control [5-6]. Moreover, ANN identification of turbogenerators in a multi-machine power system has also been reported [7].

In this paper, the electric power grid is modeled using artificial neural networks and used in the development of neurocontrollers based on derivative adaptive critics, to replace the conventional automatic voltage regulators (AVRs) and turbine governors. With derivative adaptive critics, optimal neurocontrollers can be designed by using pre-recorded data from the power system operation, and offline training, before allowing the neural network to control the generators. With adaptive critics, the computational load of online training is therefore avoided. The method presented in this paper can therefore be used in the development of neurocontrollers to be retrofitted to existing plants.

A three-machine laboratory power system example is simulated, with neurocontrollers on two generators. The third generator is the infinite bus, with a fixed voltage

and frequency. The simulation results show that both voltage regulation and system stability enhancement can be achieved with this proposed neurocontroller, regardless of the system operating conditions and types of disturbances.

2 Electric Power Grid

The multi-machine laboratory power system in figure 1 is modeled in the MATLAB/SIMULINK environment using the Power System Blockset (PSB) [8]. Each machine is represented by a seventh order model. There are three coils on the d-axis and two coils on the q-axis and the stator transient terms are not neglected. A three machine five-bus power system is chosen, to illustrate the effectiveness of the adaptive critic based controllers. The power system in figure 1 consists of two micro-generators.

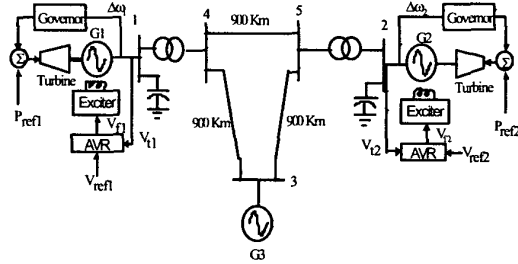


Figure 1: Multimachine Power System Model

Each of the 3 kW, 220 V, three phase micro-generator was designed to have all its per-unit parameters, except the field winding resistance, the same as those normally expected of a 1000 MW generator. The parameters of the micro-generators, determined by the IEEE standards are given in Table 1 [9]. A time constant regulator is used on each micro-generator to insert negative resistance in series with the field winding circuit, in order to reduce the actual field winding resistance to the correct per-unit value.

The conventional AVR and exciter combination transfer function block diagram is similar for both generators and is shown in figure 2 and the time constants are given in Table 2. The exciter saturation factor S_e is given by

$$S_e = 0.6093 \exp(0.2165V_{fd}) \quad (1)$$

T_{v1} , T_{v2} , T_{v3} and T_{v4} are the time constants of the PID voltage regulator compensator; T_{v5} is the input filter time constant; T_e is the exciter time constant; K_{av} is the AVR gain; V_{fdm} is the exciter ceiling; and, V_{ma} and V_{mi} are the AVR maximum and minimum ceilings.

Table 1: Micro-Generator Parameters.

$T_{d0}' = 4.50$ s	$X_d' = 0.205$ pu	$R_s = 0.006$
$T_{d0}'' = 33$ ms	$X_d'' = 0.164$ pu	$H = 5.68$
$T_{q0}'' = 0.25$ s	$X_q = 1.98$ pu	$F = 0$
$X_d = 2.09$ pu	$X_q'' = 0.213$ pu	$p = 2$

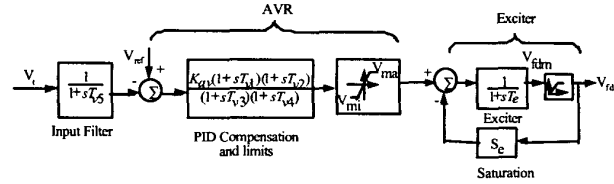


Figure 2: Block Diagram of the AVR and Exciter Combination.

Table 2: AVR and Exciter Time Constants.

T_{v1}	0.616 s	T_{v4}	0.039 s
T_{v2}	2.266 s	T_{v5}	0.0235 s
T_{v3}	0.189 s	T_e	0.47 s

A separately excited 5.6 kW dc motor is used as a prime mover, called the micro-turbine, to drive each of the micro-generators. The torque-speed characteristic of the dc motor is controlled to follow a family of rectangular hyperbola for different positions of the steam valve, as would occur in a real typical high pressure (HP) turbine cylinder. The three low pressure (LP) cylinders' inertia are represented by appropriately scaled flywheels. The micro-turbine and the governor transfer function block diagram is shown in figure 3, where, P_{ref} is the turbine input power set point value, P_m is the turbine output power, and $\Delta\omega$ is the speed deviation. The turbine and governor time constants are given in Table 3.

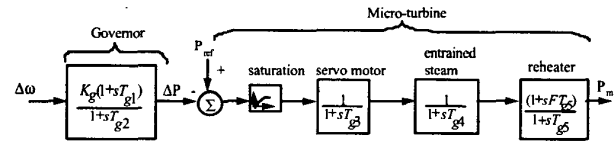


Figure 3: Block Diagram of the Micro-Turbine and Governor Combination.

Table 3: Micro-Turbine and Governor Time Constants

Phase advance compensation, T_{g1}	0.264
Phase advance compensation, T_{g2}	0.0264
Servo time constant, T_{g3}	0.15
Entrained steam delay, T_{g4}	0.594
Steam reheat time constant, T_{g5}	2.662
pu shaft output ahead of reheater, F	0.322

3 Derivative Adaptive Critics' Based Neurocontrollers

Adaptive Critic Designs (ACDs) are neural network designs capable of optimization over time under conditions of noise and uncertainty. A family of ACDs was proposed by Werbos [10] as a new optimization technique combining concepts of reinforcement learning and approximate dynamic programming. For a given series of control actions, that must be taken in sequence, and not knowing the quality of these actions until the end of the sequence, it is impossible to design an optimal controller using traditional supervised learning.

Dynamic programming prescribes a search which tracks backward from the final step, rejecting all suboptimal paths from any given point to the finish, but retains all other possible trajectories in memory until the starting point is reached. However, many paths which may be unimportant, are nevertheless also retained until the search is complete. The result is that the procedure is too computationally demanding for most real problems. In supervised learning, an ANN training algorithm utilizes a desired output and, comparing it to the actual output, generates an error term to allow learning. For an MLP type ANN the backpropagation algorithm is typically used to get the necessary derivatives of the error term with respect to the training parameters and/or the inputs of the network. However, backpropagation can be linked to reinforcement learning via a network called the *Critic* network, which has certain desirable attributes.

Critic based methods remove the learning process one step from the control network (traditionally called the "Action network" or "actor" in ACD literature), so the desired trajectory or control action information is not necessary. The critic network learns to approximate the cost-to-go or strategic utility function, and uses the output of an action network as one of its inputs directly or indirectly. When the critic network learns, backpropagation of error signals is possible along its input pathway from the action network. To the backpropagation algorithm, this input pathway looks like just another synaptic connection that needs weight adjustment. Thus, no desired signal is needed. All that is required is a desired cost function J given in eq. (2).

$$J(t) = \sum_{k=0}^{\infty} \gamma^k U(t+k) \quad (2)$$

where γ is a discount factor for finite horizon problems ($0 < \gamma < 1$), and $U(\cdot)$ is the utility function or local cost.

The Critic and the Action networks, can be connected together directly (Action-dependent designs) or through

an identification model of a plant (Model-dependent designs). There are three classes of implementations of ACDs called Heuristic Dynamic Programming (HDP), Dual Heuristic Programming (DHP), and Globalized Dual Heuristic Dynamic Programming (GDHP), listed in order of increasing complexity and power [11]. This paper presents the DHP model dependent design, and compares its performance against the results obtained using conventional PID controllers.

The critic network is trained forward in time, which is of great importance for real-time operation. DHP has a critic network which estimates the derivatives of J with respect to a vector of observables of the plant, ΔY . The critic network learns minimization of the following error measure over time:

$$\|E\| = \sum_i E^T(t)E(t) \quad (3)$$

where

$$E(t) = \frac{\partial J[\Delta Y(t)]}{\partial \Delta Y(t)} - \gamma \frac{\partial J[\Delta Y(t+1)]}{\partial \Delta Y(t)} - \frac{\partial U(t)}{\partial \Delta Y(t)} \quad (4)$$

where $\partial(\cdot)/\partial \Delta Y(t)$ is a vector containing partial derivatives of the scalar (\cdot) with respect to the components of the vector ΔY . The critic network's training is more complicated than in HDP since there is a need to take into account all relevant pathways of backpropagation as shown in figure 4, where the paths of derivatives and adaptation of the critic are depicted by dashed lines.

In DHP, application of the chain rule for derivatives yields

$$\frac{\partial J(t+1)}{\partial \Delta Y_j(t)} = \sum_{i=1}^n \lambda_i(t+1) \frac{\partial \Delta Y_i(t+1)}{\partial \Delta Y_j(t)} \quad (5)$$

$$\sum_{k=1}^m \sum_{i=1}^n \lambda_i(t+1) \frac{\partial \Delta Y_i(t+1)}{\partial A_k(t)} \frac{\partial A_k(t)}{\partial \Delta Y_j(t)}$$

where $\lambda_i(t+1) = \partial J(t+1)/\partial \Delta Y_i(t+1)$, and n, m are the numbers of outputs of the model and the action networks, respectively. By exploiting eq. (5), each of n components of the vector $E(t)$ from eq. (4) is determined by

$$E_j(t) = \frac{\partial J(t)}{\partial \Delta Y_j(t)} - \gamma \frac{\partial J(t+1)}{\partial \Delta Y_j(t)} - \frac{\partial U(t)}{\partial \Delta Y_j(t)} \quad (6)$$

$$- \sum_{k=1}^m \frac{\partial U(t)}{\partial A_k(t)} \frac{\partial A_k(t)}{\partial \Delta Y_j(t)}$$

The action network is adapted in figure 5 by propagating $\lambda(t+1)$ back through the model to the action.

The goal of such adaptation can be expressed as:

$$\frac{\partial U(t)}{\partial A(t)} + \gamma \frac{\partial J(t+1)}{\partial A(t)} = 0 \quad \forall t \quad (7)$$

The weights' update expression is:

$$\Delta W_A = -\alpha \left[\frac{\partial U(t)}{\partial A(t)} + \gamma \frac{\partial J(t+1)}{\partial A(t)} \right]^T \frac{\partial A(t)}{\partial W_A} \quad (8)$$

where α is a positive learning rate.

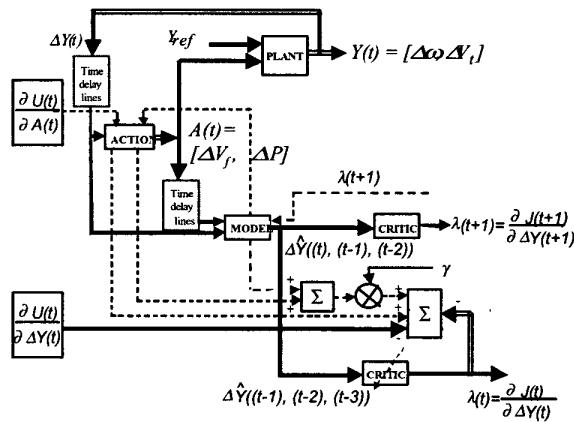


Figure 4: DHP Critic Network Adaptation

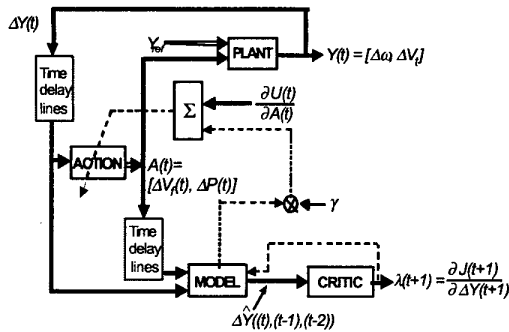


Figure 5: DHP Action Network Adaptation

4 Three Artificial Neural Networks -Model, Critic and Action

Neurocontrollers are designed to replace the AVRs and governors on generator G1 and G2, and therefore ANN models of generator G1 and G2, and the networks to which they are connected are obtained as described in

[7]. The ANN model in figures 4 & 5 is a three layer feedforward network with twelve inputs, a single hidden layer of fourteen neurons and two outputs. The inputs to the ANN are the *deviation* of the *actual* power ΔP to its turbine, the *deviation* of the *actual* field voltage ΔV_f to its exciter, the *deviation* of the *actual* speed $\Delta \omega$ and the *deviation* of the *actual* RMS terminal voltage ΔV_t of its generator. These four inputs are also delayed by the sample period of 10 ms and, together with eight previously delayed values, form twelve inputs altogether. For this set of inputs, the outputs are the *estimated* speed deviation $\Delta \hat{\omega}$ and the *estimated* terminal voltage deviation $\Delta \hat{V}_t$, of the generator.

The critic network in figures 4 & 5 is also a three layer feedforward network with six inputs, thirteen hidden neurons and, two outputs. The inputs to the critic network are the speed *deviation* $\Delta \omega$ and terminal voltage *deviation* ΔV_t . These inputs are time delayed by a sample period of 10 ms, and together with the four previously delayed values, form the six inputs for the critic network. The outputs of the critic are the derivatives of the J function with respect to the output states of the generators.

The action network in figures 4 & 5 is also a three layer feedforward network with six inputs, a single hidden layer with ten neurons and a single output. The inputs are the generator's *actual* speed and *actual* terminal voltage deviations, $\Delta \omega$ and ΔV_t , respectively. Each of these inputs is time delayed by 10 ms and, together with four previously delayed values, form the six inputs. The output of the action network (neurocontroller), $A(t) = [\Delta V_f, \Delta P]$, the *deviation* in the field voltage, which augments the input to the generator's exciter and the deviation in the power, which augments the input to the generator's turbine.

5 Simulation of the Neurocontrollers and Results

The training procedure for the critic and action networks is similar to adaptive critic designs for SMIB [6]. It consists of two training cycles: the critic's and the action's. The critic's adaptation is done initially with a pretrained action network, to ensure that the whole system, consisting of the ACD and the power system, remains stable. The action network is pretrained on a linearized model of the generator. The action is trained further while keeping the critic network parameters fixed. This process of training the critic and the action one after the other is repeated until an acceptable performance is achieved. The ANN model parameters are assumed to have converged globally during its offline

training [7] and, it is not adapted concurrently with the critic and action networks.

A discount factor γ of 0.5 and the utility function given in eq. (9) are used in the Bellman's equation (eq. (2)) for the training of the critic network (eqs. (4)) and the action network (eq. (7)). Once the critic network's and action network's weights have converged, the action network (neurocontroller) is connected to the generator G1 (figure 6). A similar procedure is carried out in developing G2's neurocontroller.

$$U(t) = [4\Delta V(t) + 4\Delta V(t-1) + 16\Delta V(t-2)]^2 + [0.4\Delta\omega(t) + 0.4\Delta\omega(t-1) + 0.16\Delta\omega(t-2)]^2 \quad (9)$$

At two different operating conditions and three different disturbances, the transient performance of the neurocontrollers are compared, with that of conventional controllers [12] (whose parameters are carefully tuned for the first set of the operating condition given in Appendix).

3% Step change in V_{11} at first operating condition

At the first operating condition (Appendix), a 3% increase occurs in the desired terminal voltage of G1. Figures 7 and 8 show that the neurocontroller ensures no overshoot on the terminal voltage and provides superior speed deviation damping unlike with the AVR and governor combination.

5% Step change in V_{12} at second operating point

At the second operating condition (Appendix), a 5% increase occurs in the desired terminal voltage of G2. Figures 9 and 10 show that the neurocontroller again provides the best damping, which proves that the neurocontroller has learned and adapted itself to the new operating condition. In fact, figure 10 shows signs of an inter-area mode starting up at about 4.5 seconds, and the neurocontroller is far more successful in damping this, than the conventional controllers.

Three phase short circuit

At the second operating condition (Appendix), a 100 ms short circuit occurs halfway between buses 3 and 4 (figure 6). Figure 11 shows that the neurocontroller again has better damping on the speed deviation of G1 and also on the terminal voltage (though not shown to conserve space).

All these results show that at operating conditions different from the one at which the AVRs and governors were tuned, and for large disturbances, their performance has degraded. The neurocontrollers on the other hand have given excellent performance under all the

conditions tested. Many more tests were done to confirm this.

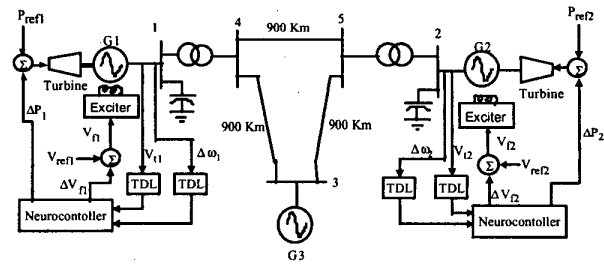


Figure 6: Multi-machine Power System with Neurocontrollers on Generators G1 and G2

6 Conclusions

A new method, based on derivative adaptive critics for the design of neurocontrollers for generators in a multi-machine power system has been presented. All control variables are based on local measurements, thus, the control is decentralized. The results show that the neurocontrollers ensure a superior transient response throughout the system, for different disturbances and different operating conditions, compared to the conventional controllers, the AVRs and governors. Further studies on the practical implementation of these neurocontrollers on multiple generators on a laboratory system are currently in progress and preliminary results look encouraging. The success of the neurocontrollers are based on using deviation signals, and having a complete nonlinear model of the system. The use of such intelligent nonlinear controllers will allow power plants on the electric power grid to operate closer to their stability limits.

7 References

- [1] Q.Lu and Y.Sun, "Nonlinear stabilizing control of multimachine systems," *IEEE Trans. Power System*, vol. 4, 1989, pp. 236-241.
- [2] Y.Wang, D.J.Hill, L.Gao and R.H.Middleton, "Transient stability enhancement and voltage regulation of power system", *IEEE Trans. Power System*, vol. 8, 1993, pp. 620-627.
- [3] Z.Qiu, J.F.Dorsey, J.Bond and J.D.McCalley, "Application of robust control to sustained oscillations in power systems", *IEEE Trans. Circuits System*, I, vol. 39, 1992, pp. 470-476.
- [4] G.K.Venayagamoorthy and R.G.Harley, "A continually online trained artificial neural network identifier for a turbogenerator", *Proceedings of 1999 IEEE International Electric Machines and Drives Conference*, 0-7803-5293-9/99, pp. 404 - 406.
- [5] G.K.Venayagamoorthy and R.G.Harley, "Experimental studies with a continually online trained artificial neural network controller for a turbogenerator", *Proceedings of the*

International Joint Conference on Neural Networks, IJCNN 1999, vol. 3, pp. 2158-2163.

[6] G.K.Venayagamoorthy, R.G.Harley, and D.C.Wunsch, "Comparison of a heuristic dynamic programming and a dual heuristic programming based adaptive critics neurocontroller for a turbogenerator", *Proceedings of the International Joint Conference on Neural Networks, IJCNN 2000*, paper no. 660.

[7] G.K.Venayagamoorthy, R.G.Harley, and D.C.Wunsch, "Adaptive neural network identifiers for effective control of turbogenerators in a multimachine power system", *Proceedings of the IEEE PES Winter Meeting 2001*, paper no. 2001WM154.

[8] G.Sybille, P.Brunelle, R.Champagne, L.Dessaint and Hoang Lehu, *Power system blockset version 2.0*, Mathworks Inc., 2000.

[9] D.J.Limebeer, R.G.Harley and S.M.Schuck, "Subsynchronous Resonance of Koeberg Turbogenerators and of a Laboratory Micro-alternator System", *Transactions of the South African Institute of Electrical Engineers*, November 1979, pp. 278-297.

[10] P.Werbo, *Approximate dynamic programming for real-time control and neural modeling*, in Handbook of Intelligent Control, White and Sofge, Eds., Van Nostrand Reinhold, ISBN 0-442-30857-4, pp 493 – 525.

[11] D.Prokhorov, D Wunsch, "Adaptive Critic Designs", *IEEE Trans. on Neural Networks*, vol. 8, no.5, pp 997-1007.

[12] W.K.Ho, C.C.Hang, L.S.Cao, "Tuning of PID controllers based on gain and phase margin specifications", *Proceedings of the 12th Triennial World Congress on Automatic Control*, 1993, pp. 199 –202.

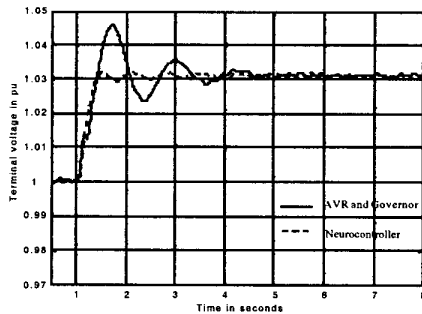


Figure 7: Terminal Voltage of Generator G1 for a 3% Step Change in its Desired Terminal Voltage

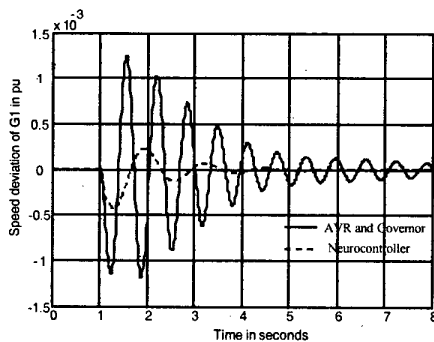


Figure 8: Speed Deviations of Generator G1 for a 3% Step Change in its Desired Terminal Voltage

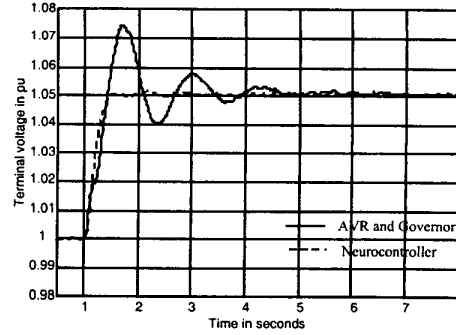


Figure 10: Terminal Voltage of Generator G2 for a 5% Step Change in its Desired Terminal Voltage

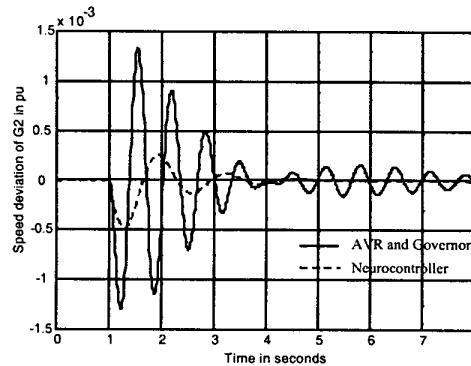


Figure 10: Speed Deviation of Generator G2 for a 5% Step Change in its Desired Terminal Voltage

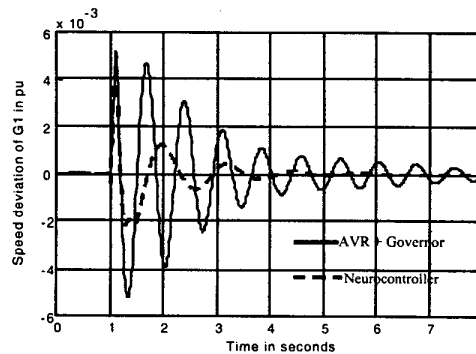


Figure 11: Speed Deviation of Generator G1 for a 100 ms 3-Phase Short Circuit between bus 3 and 4

8 Appendix

	Condition one		Condition two	
	G1	G2	G1	G2
P_e (pu)	0.200	0.200	0.3000	0.300
Q (pu)	-0.0216	-0.0218	-0.0493	-0.0341
V_i (pu)	1	1	1	1